JOURNAL OF VIROLOGY, Jan. 2005, p. 997–1007 Vol. 79, No. 2
0022-538X/05/$08.00+0 doi:10.1128/JVI.79.2.997–1007.2005

Incorporation of Three Endocytosed Varicella-Zoster Virus Glycoproteins, gE, gH, and gB, into the Virion Envelope

Lucie Maresova, Tracy Jo Pasieka, Elizabeth Homan, Erick Gerday, and Charles Grose*

Department of Pediatrics and Central Microscopy Research Facility, University of Iowa, Iowa City, Iowa

Received 23 May 2004/Accepted 25 August 2004

The cytoplasmic tails of all three major varicella-zoster virus (VZV) glycoproteins, gE, gH, and gB, harbor functional tyrosine-based endocytosis motifs that mediate internalization. The aim of the present study was to examine whether endocytosis from the plasma membrane is a cellular route by which VZV glycoproteins are delivered to the final envelopment compartment. In this study, we demonstrated that internalization of the glycoproteins occurred in the first 24 h postinfection but was reduced later in infection. Using surface biotinylation of VZV-infected cells followed by a glutathione cleavage assay, we showed that endocytosis was independent of antibody binding to gE, gH, and gB. Subsequently, with this assay, we demonstrated that biotinylated gE, gH, and gB retrieved from the cell surface were incorporated into nascent virus particles isolated after density gradient sedimentation. To confirm and extend this finding, we repeated the above sedimentation step and specifically detected envelopes decorated with Streptavidin-conjugated gold beads on a majority of complete virions through examination by transmission electron microscopy. In addition, a gE-gI complex and a gE-gH complex were found on the virions. Therefore, the above studies established that VZV subsumed a postendocytosis trafficking pathway as one mechanism by which to deliver viral glycoproteins to the site of virion assembly in the cytoplasm. Furthermore, since a recombinant VZV genome lacking only endocytosis-competent gE cannot replicate, these results supported the conclusion that the endocytosis-envelopment pathway is an essential component of the VZV life cycle.

Endocytosis has now been demonstrated for numerous herpesvirus type 1 glycoproteins in transfected cell systems. In addition to gE of varicella-zoster virus (VZV), herpes simplex virus type 1 (HSV-1) gE and pseudorabies virus (PrV) gE undergo endocytosis (2, 3, 47, 58, 57). Also, PrV gB and human cytomegalovirus (HCMV) gB internalize in transfected cells (51, 58, 60). Unlike the situation for other human herpesviruses, the predominant VZV glycoprotein present on the envelope of the mature virion is gE (4, 23, 44). The gE protein traffics from the endoplasmic reticulum (ER) through the Golgi apparatus, where it is extensively processed, to the outer cell membrane. Both the ectodomain and the endodomain of gE have important functions. Based on the fact that a single point mutation in the VZV-MSP gE ectodomain changes the VZV-MSP egress pattern from a typical "viral highway" phenotype to a diffuse pattern similar to that observed in HSV-1-infected cells (53, 54), the ectodomain is likely to be critical for determining virus-cell interactions of mature virions.

VZV gE endocytosis is mediated by a YAGL sequence located in the cytoplasmic tail of the protein (47). This sequence fits the consensus tyrosine-based YXXΦ endocytosis motif (where Y is tyrosine, X is any amino acid, and Φ is any bulky hydrophobic amino acid) (6). Recycling of gE back to the plasma membrane postendocytosis has been demonstrated, but there is also a pathway for gE to traffic to the *trans*-Golgi network (TGN) postendocytosis (2, 47). The TGN pathway is mediated by a cluster of acidic amino acids in the gE cytoplasmic tail (2, 27, 61, 68). The acidic cluster of gE interacts with the connector protein, phosphofurin acidic cluster sorting protein 1 (PACS-1), and directs VZV gE from endosomes to the TGN, a proposed site of tegument assembly and virion envelopment (10, 61, 64). Phosphorylation within this acidic cluster motif mediates the PACS-1 interaction (17, 55). VZV gE is phosphorylated on its cytoplasmic tail (27, 43, 45, 66). In addition, differential phosphorylation of the gE acidic cluster targets endocytosed gE to either the TGN or the cell surface, thereby increasing virus assembly or cell-to-cell spread, respectively (38).

Like gE, VZV gI also contains in its cytoplasmic tail trafficking motifs that mediate similar functions; however, the motifs are different. A dileucine motif mediates gI endocytosis (46), and a threonine at position 338 is important for TGN targeting (63). VZV gE and gI form a complex in infected cells or when cotransfected. In addition, complex formation has been found to increase the efficiency of endocytosis of gE-gI over that of gE or gI alone (46). Complex formation between gE and gI is also able to direct the internalization of a gE endocytosis-deficient mutant, a finding which suggests that the gI motif may be more efficient than the gE motif (46).

VZV gB is the second most abundant VZV glycoprotein and is also the most conserved among the herpesvirus glycoproteins (41). The gB protein contains three potential endocytosis motifs: two tyrosine-based motifs and one dileucine-type motif. The C terminus-proximal tyrosine motif (YSRV) in VZV gB is most responsible for endocytosis, while the transmembrane domain-proximal tyrosine motif (YMTL) is responsible for

* Corresponding author. Mailing address: University of Iowa Hospital/2501 JCP, 200 Hawkins Dr., Iowa City, IA 52242. Phone: (319) 356-2270. Fax: (319) 356-4855. E-mail: charles-grose@uiowa.edu.

ER-to-TGN targeting (34, 35). VZV gH is the third most abundant glycoprotein and is the second most conserved. Endocytosis of the gH protein is mediated by a YNKI tyrosine motif in its short cytoplasmic tail (49, 50). In addition, gH is internalized in a clathrin-dependent manner similar to that of gE, gI, and gB (34, 46, 47).

Since endocytosis can target viral glycoproteins to the TGN, the proposed site of viral assembly, one attractive hypothesis is that endocytosis is required for delivering viral glycoproteins to the site of final envelopment (8, 40). Endocytosis of several HCMV surface proteins, including gB, most likely plays a role in targeting these proteins to the organelle of virion assembly (18, 19, 51). However, inhibition of HCMV gB endocytosis had a variable effect on virus release or the production of infectious virions, depending on the study (5, 36, 51). These data, considered together with the observation that PrV gE endocytosis apparently is not required for incorporation (57, 58), raise a question about the role of glycoprotein endocytosis in viral assembly. VZV still may be an important model because it has the smallest genome of the human herpesviruses with the fewest glycoproteins (11). In contrast to PrV gE, VZV gE is an essential glycoprotein that cannot be deleted from the genome (39). Even more importantly, a recent report demonstrated that a single mutation of just the gE YAGL endocytosis motif in a otherwise complete recombinant virus halted replication altogether (41). Because gE endocytosis appears to be an essential component of the VZV life cycle, the postendocytosis trafficking of gE as well as two other essential glycoproteins, gH and gB, in infected cells was investigated in detail.

MATERIALS AND METHODS

Cells and viruses. A human melanoma cell line (Mewo) highly permissive for VZV infection was maintained as previously reported (24, 28). Propagation of the VZV-32 strain (GenBank accession no. AH010537) was performed as previously described (24, 54). Monolayers inoculated with VZV-infected cells were processed 24 or 48 h postinfection (hpi) as described below.

Antibodies and fluoroprobes. Murine monoclonal antibody (MAb) 3B3 recognizes a well-characterized linear epitope in the ectodomain of gE (25, 32, 54). Murine MAb 169 and MAb 711 are directed against gE (54). Murine MAb 258 is a conformation-dependent anti-gH MAb specific for mature and immature glycosylated gH but not for the nonglycosylated immature form (12, 13). Murine MAb 206 recognizes only a conformation-dependent epitope on the fully mature form of gH (42). Murine MAb 6B5 and MAb 158 are directed against gI and gB, respectively (44, 65). Human MAb V1 is directed against gB (56), while human MAb Ti-57 recognizes gH (56). An additional murine anti-gB MAb and an additional murine anti-gH MAb were purchased from Biodesign. The Biodesign anti-gH MAb recognizes three closely migrating glycoprotein bands on Western blots (50). All fluorescent probes were purchased from Molecular Probes, and they included the Alexa 488-fluoroconjugated secondary antibody goat anti-mouse immunoglobulin G (heavy and light chains) and TOTO-3 for DNA staining.

Assay of glycoprotein endocytosis by laser scanning confocal microscopy. Glycoprotein endocytosis was investigated with immunofluorescence labeling as previously described (13, 49). The samples were viewed with a Zeiss 510 laser scanning confocal microscope.

Biotinylation of cell surface glycoproteins in VZV-infected cells. Cell monolayers were inoculated with VZV-32-infected cells. The cell surface expression of glycoproteins was investigated after biotinylation with NHS-LC-biotin (Pierce, Rockford, Ill.) as previously described (50). For the detection of VZV gE and gI, a 3-cm^2 monolayer per sample was used; a 12-cm^2 monolayer per sample was used for the detection of gH and gB. The labeled monolayers were harvested in radioimmunoprecipitation assay buffer (0.01 M Tris-HCl [pH 7.4], 0.15 M NaCl, 1% NP-40, 1% deoxycholate, 0.1% sodium dodecyl sulfate [SDS]) with inhibitors (1 mM phenylmethylsulfonyl fluoride, 1 mM benzamidine, 1 mM leupeptin, and 0.025 trypsin inhibition unit each of aprotinin and type 1-S soybean trypsin inhibitor). After immunoprecipitation of specific glycoproteins with either anti-gE, anti-gI, anti-gH, or anti-gB MAb, samples were loaded onto an 8% polyacrylamide gel for SDS-polyacrylamide gel electrophoresis (PAGE) under nonreducing conditions. Immunoprecipitated biotinylated glycoproteins were detected with Streptavidin-horseradish peroxidase (HRP) by Western blotting (49, 54).

Endocytosis of VZV glycoproteins assayed by biotinylation in infected cells. Cultured cells were inoculated with VZV-32-infected cells for 24 or 48 hpi, and endocytosis was investigated as previously described but with some modifications (49). Generally, we used one 25-cm^2 monolayer per sample. After surface biotinylation with Sulfo-NHS-SS-biotin (Pierce), infected monolayers were incubated for various times at 37°C to allow endocytosis of the glycoproteins. Internalization was stopped by cooling on ice. Cells were washed and incubated three times for 20 min each time with freshly prepared glutathione (GSH) buffer (60 mg of GSH/ml [pH 8.0], 83 mM NaCl, 1.1 mM $CaCl_2$, 1.1 mM $MgCl_2$) at 4°C to remove any remaining biotin label from proteins present at the cell surface. After several washes, the cells were harvested. Immunoprecipitation was performed with MAb 3B3 to detect gE, MAb Ti-57 to detect gH, or anti-gB MAb 158. Samples were separated by SDS–8% PAGE under nonreducing conditions, and internalized biotinylated glycoproteins were detected with Streptavidin-HRP by Western blotting.

One point that has been noted since the first description of this technique (7) is that uncleaved samples always stain much more intensely than cleaved samples. Thus, this method does not provide a quantitative estimation of the relative percentages of cell surface glycoproteins internalized. One potential explanation is that GSH cleavage of the disulfide-linked biotin remaining at the cell surface, after allowing for endocytosis to occur, decreases the signal in the internalized proteins. In some studies in which this method was used, precleavage lanes in each biotinylation experiment were not shown (31).

Incorporation of endocytosed VZV glycoproteins into virion particles. The levels of glycoproteins incorporated into VZV virions after endocytosis from the cell surface were determined by surface biotinylation as described above but with modifications. An uninfected monolayer was inoculated at a 1:2 ratio of infected to uninfected cells and was incubated for 24 h at 37°C. Cultures were washed four times with 10 mM borate buffer (pH 8.8) containing 0.1 M NaCl to remove any remaining virus inoculum. After surface biotinylation with cleavable Sulfo-NHS-SS-biotin, the monolayer was incubated for 5 h at 37°C to allow for endocytosis and virion formation. Internalization was stopped, and cells were washed and incubated three times for 20 min each time with GSH buffer. After several washes, the cells were harvested, sonicated, and resuspended in sorbitol buffer (10% sorbitol, 0.05 M Tris-Cl [pH 7.4], 0.001 M $MgCl_2$). The cell-free virus then was layered onto a linear gradient of potassium tartate (KT) and glycerol in TE buffer (0.002 M EDTA, 0.002 M Tris-Cl [pH 7.4]) (28). After centrifugation at 25,000 rpm for 18 h at 4°C in a Beckman SW27 rotor, the virion band was removed and layered onto another KT-glycerol gradient. After a second sedimentation, virus was again found in a particulate band. The virion band was washed twice with TE buffer at 26,000 rpm for 1 h, and the pellet was resuspended in TE buffer, after which it was mixed with an equal volume of 2× radioimmunoprecipitation assay buffer. Immunoprecipitation was performed with anti-gE MAb 3B3, anti-gH MAb Ti-57, or anti-gB MAb 158. Samples were separated by SDS–8% PAGE under nonreducing conditions, and biotinylated glycoproteins were detected with Streptavidin-HRP by Western blotting.

For detection of total gE, gH, or gB in virion fractions and infected cell lysates, immunoblotting was performed with anti-gE MAb 3B3 (1:10,000), anti-gH MAb (1:2,000; Biodesign), or anti-gB MAb (1:500; Biodesign), respectively. Both virion fractions and cell lysates were also tested for the presence of the TGN marker, TGN-46 protein, or transferrin receptor (TfR). Reagents included a sheep anti-TGN-46 MAb (1:1,000; Santa Cruz Biotechnology) and a rabbit polyclonal anti-TfR antibody (1:100; (Santa Cruz Biotechnology).

Transmission electron microscopy (TEM). VZV-32-infected cells were harvested, sonicated, and resuspended in sorbitol buffer. The VZV virions isolated by centrifugation in two successive KT-glycerol gradients were resuspended in TE buffer, placed on copper grids with carbon-coated Formvar, and negatively stained with 1% ammonium molybdate for 60 s. The samples were viewed with a Hitachi H-7000 transmission electron microscope at an accelerating voltage of 75,000 V (28, 30).

Imaging after decoration of virions with gold beads. To specifically detect biotinylated VZV virions, an aliquot of a purified virion fraction was collected after the incorporation assay and examined by TEM. The sample was fixed with 2.5% glutaraldehyde in 0.1 M cacodylate buffer, placed on a copper-collodion-carbon-coated grid for 15 min at 24°C, and washed with PBS. In the next step, the sample was incubated with Aurion Streptavidin-conjugated 10-nm gold beads (Electron Microscopy Sciences) at a dilution of 1:75 in PBS for 45 min at 24°C. After several washes, the sample was negatively stained with 3% ammonium

molybdate and viewed with a Hitachi H-7000 transmission electron microscope at an accelerating voltage of 75,000 V.

As a second method for detecting biotinylated VZV virions, an aliquot of the purified virion fraction was placed on a copper-Formvar-carbon grid for 15 min at 24°C and incubated with antibiotin Aurion-conjugated ultrasmall gold beads (0.8 nm; Electron Microscopy Sciences) at a dilution of 1:10 in 0.1% Aurion BSA-c buffer (Electron Microscopy Sciences) for 2 h at 37°C. After several washes with 0.1% Aurion BSA-c buffer, silver enhancement was performed with an Aurion EM silver enhancement kit (Electron Microscopy Sciences). Silver enhancement is required in order to visualize the ultrasmall gold beads. After further washes with H_2O, the sample was negatively stained with 1% ammonium molybdate and viewed with a Hitachi H-7000 transmission electron microscope at an accelerating voltage of 75,000 V.

RESULTS

Biotinylation of and endocytosis in VZV-infected cells. As evidence for endocytosis and recycling of VZV glycoproteins has accumulated (49, 50), we postulated that all VZV glycoproteins with internalization motifs were incorporated into the virion envelope. To test this hypothesis, we first documented the localization of viral glycoproteins on the surface of infected cells by biotinylation. For this analysis, biotinylated glycoproteins were immunoprecipitated with specific MAbs and then detected under nonreducing conditions with Streptavidin-HRP. At least two MAbs against different forms (mature and immature) of each glycoprotein were selected to ensure that glycoprotein expression was accurately assessed. The results demonstrated that gE, gH, and gB were easily detected on the cell surface by this method (data not shown). As previously observed, gE was invariably the most abundant VZV glycoprotein.

Because endocytosis of VZV glycoproteins has not been investigated in as much detail in infected cells as under transfection conditions, we determined whether endocytosis was inhibited late in infection. VZV infection results in the formation of multinucleated syncytia and thus increases the fragility of monolayers, one reason for the technical difficulty in performing these assays. In prior experiments, all four VZV glycoproteins, gE, gI, gH, and gB, were endocytosed at 24 hpi in VZV-infected cells (49). The next set of experiments was designed to determine whether viral glycoproteins continued to be internalized from the plasma membrane of infected cells at later time points. To this end, infected monolayers were processed for the immunofluorescence endocytosis assay at 48 hpi (Fig. 1A). At this point, syncytium formation was heavily advanced; therefore, most syncytia consisted of more than 25 fused cells. As a positive control, infected monolayers assayed at 24 hpi were used.

At the beginning of the endocytosis assay, only the glycoproteins on the cell surface were labeled with primary antibody. Samples never returned to 37°C had no glycoprotein visible inside single cells and syncytia (data not shown). As expected, at 24 hpi and after 60 min of incubation at 37°C, all VZV glycoproteins were internalized from the plasma membrane to the interior of both syncytia and infected single cells (Fig. 1A). In contrast, the results obtained at 48 hpi demonstrated a markedly diminished level of endocytosis for all glycoproteins in large syncytia (>25 nuclei) (Fig. 1A). As previously mentioned, all confocal experiments were carried out with at least two MAbs against each glycoprotein to ensure that all forms were detectable.

The next set of experiments was designed to further extend the biotin endocytosis assay for infected cells by demonstrating the inhibition of VZV glycoprotein endocytosis at 48 hpi, as previously shown by the confocal experiments. In these experiments, an entire 25-cm^2 infected monolayer per sample was used. We began with gE, since a strong endocytosis band was detected in the transfected cell system (49). The results of the biotin endocytosis assay are shown in Fig. 1B. The 0- and 60-min samples in Fig. 1B, lanes 1 and 6, showed total cell surface biotinylation of gE before a GSH cleavage step. As described in Materials and Methods and as noted previously in other studies (7, 49), the uncleaved biotinylated samples stained very intensely with this labeling method, in particular, gE. It is also relevant that less than 33% of the cell surface gE was internalized, so that a majority of gE remained on the cell surface (47). The sample in Fig. 1B, lane 6, was included to demonstrate that gE was not degraded inside the cell after 60 min of incubation at 37°C. The results also demonstrated the coprecipitation of cell surface gI by anti-gE MAb 3B3 (Fig. 1B, lanes 1 and 6). The absence of a glycoprotein band in the 0-min sample in Fig. 1B, lane 2, demonstrated that the cleavage step removed all cell surface biotin. The 30-min, 60-min, and 20-h samples in Fig. 1B, lanes 3 to 5, were returned to 37°C for the indicated times before the cleavage step. Thus, if the tested glycoproteins were internalized, then a band would be detectable in these lanes. As expected, only minimal gE endocytosis was evident (Fig. 1B, lanes 3 to 5). Even when the film was exposed longer, little internalized gE was seen. Again, the results demonstrated a marked reduction of endocytosis in VZV syncytia at about 48 hpi.

Endocytosis of VZV gE at 24 hpi. Based on the above results, we began the biotin endocytosis assay by testing for gE internalization at 24 hpi (Fig. 2). As for the experiments shown in Fig. 2, an entire 25-cm^2 infected monolayer per sample was used. The 0-min and 1-, 6-, and 20-h samples in Fig. 2, lanes 1, 8, 9, and 10, showed total cell surface biotinylation of gE. The absence of a glycoprotein band in the 0-min sample in Fig. 2, lane 2, demonstrated that the cleavage step removed all cell surface biotin. The 1-, 3-, 5-, 6-, and 20-h samples in Fig. 2, lanes 3 to 7, were returned to 37°C for the indicated times before the cleavage step. The results indicated that gE endocytosis became evident at 1 h and continued to accumulate through the 3-h time point (Fig. 2, lanes 3 and 4).

As noted in Fig. 1, VZV gE in Fig. 2, lane 1, appeared to be overexposed. In order to visualize the internalized gE and the surface gE in the same gel, the surface gE invariably appeared overexposed. The same samples also showed coprecipitation of gE and gI. The gI band was more visible in the 1- and 3-h samples after longer exposures (data not shown). This result indicated that the glycoproteins formed a complex during endocytosis. Thus, in contrast to the assay at 48 hpi (Fig. 1B), the biotin-GSH cleavage assay successfully detected abundant gE endocytosis at 24 hpi. The samples in Fig. 2, lanes 8 to 10, were included to demonstrate that gE was not degraded during the indicated incubation times. Fig. 2, lane 11, represented a shorter exposure of lane 10 and delineated the migration of individual glycoprotein forms. Further, these data confirmed the results shown in Fig. 1, namely, that after 30 h (24 hpi plus 6 h of incubation), the amount of internalized protein was diminished (Fig. 2, lanes 6 and 7).

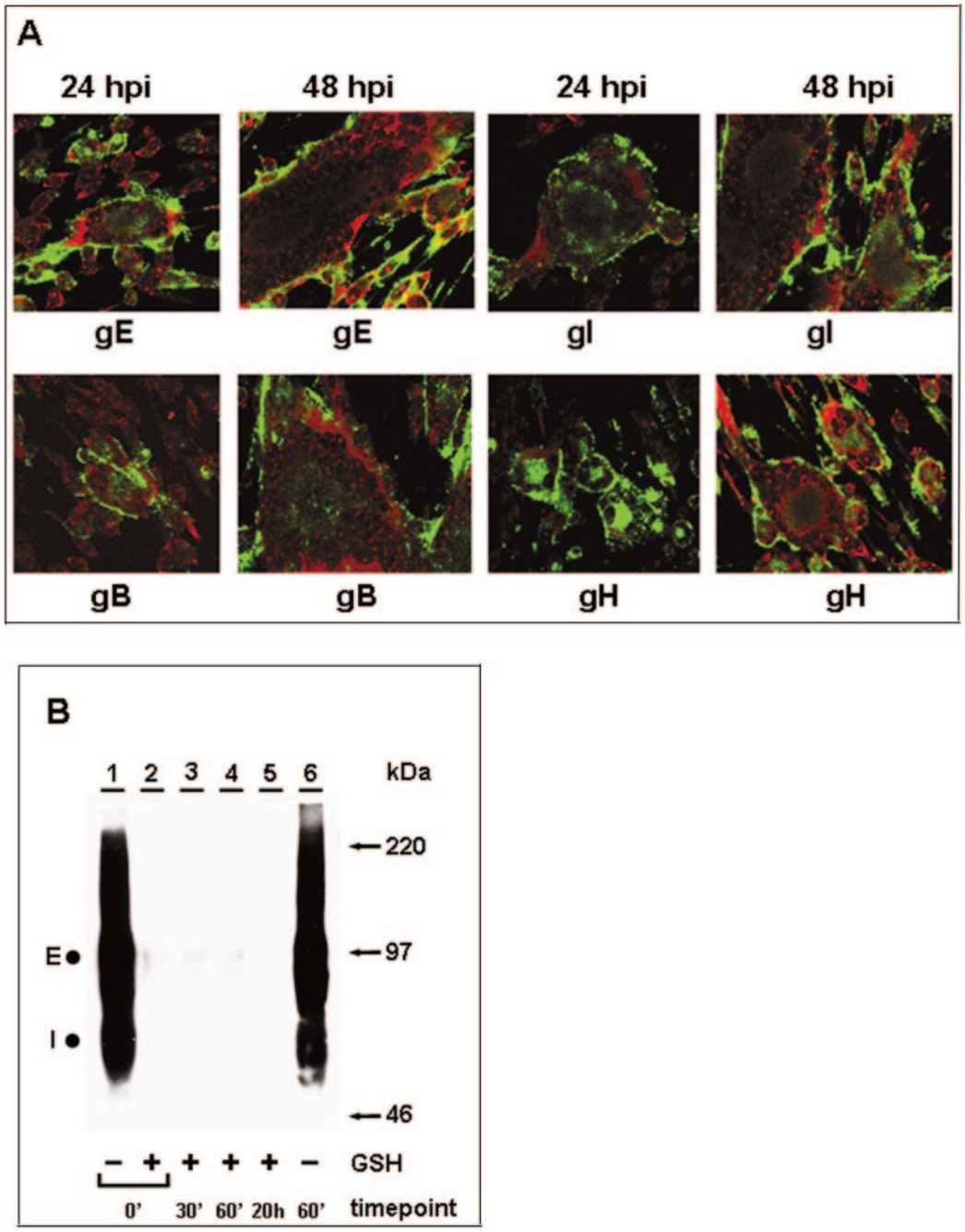

FIG. 1. Inhibition of VZV glycoprotein endocytosis during late infection. VZV-infected cells were processed for the confocal endocytosis assay as described in the text. (A) Representative micrographs of cultures at 24 and 48 hpi were examined at the 60-min endocytosis time point after labeling was done with a MAb specific for gE, gI, gB, or gH. The postendocytosis localization of VZV glycoproteins was investigated by staining with Alexa 488-fluoroconjugated goat anti-mouse immunoglobulin secondary antibody (green). In contrast to the results obtained at 48 hpi, at 24 hpi labeled glycoproteins were located at the plasma membrane and in vesicles within the cytoplasm of the syncytia. The vesicles were especially evident in smaller syncytia. Nuclei were stained with TOTO-3 (red). (B) Biotin endocytosis assay showing the inhibition of gE internalization at 48 hpi. Cells were infected for 48 h, and samples were processed for the biotin endocytosis assay as described in the text. The numbers below the gel indicate the endocytosis time points at 37°C; + and − above the numbers indicate the presence and absence of GSH treatment, respectively. Samples were separated by SDS–8% PAGE under nonreducing conditions, and internalized biotinylated glycoprotein was detected with Streptavidin-HRP by Western blotting. E and I designate the two glycoproteins. Additional controls for this assay are shown in Fig. 2. The corresponding molecular mass markers are indicated on the right.

Incorporation of cell surface biotinylated gE into VZV virions. To investigate whether endocytosed VZV glycoproteins were incorporated into virion particles, we performed the biotin-GSH cleavage assay followed by virion isolation from KT-glycerol gradients. The results of the gE incorporation assay are shown in Fig. 3. One 25-cm^2 infected monolayer was used per 0-min sample in Fig. 3, lanes 1 to 3, and per 5-h sample in lanes 4 and 5. One 75-cm^2 infected monolayer was used to

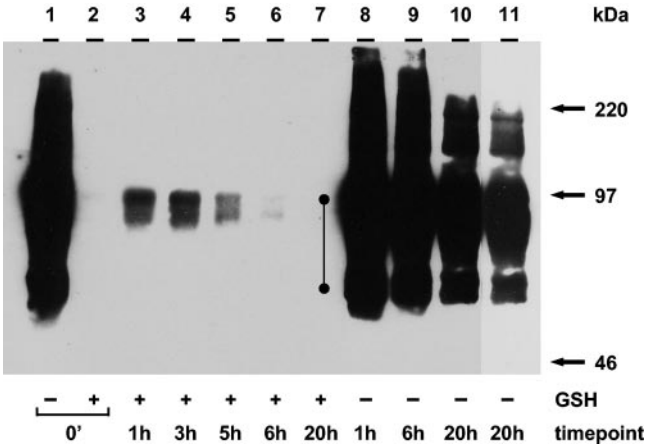

FIG. 2. Biotin endocytosis assay showing the internalization of gE at 24 hpi. Cultured cells were infected and processed for the biotin endocytosis assay as described in the text. The numbers below the gel indicate the endocytosis time points at 37°C; + and − above the numbers indicate the presence and absence of GSH treatment, respectively. After SDS-PAGE, internalized biotinylated glycoprotein was detected with Streptavidin-HRP by Western blotting. The closed circles beside lane 8 indicate gE and gI. Lane 11 represents a shorter exposure of lane 10 to confirm the migration of the individual glycoprotein forms. The corresponding molecular mass markers are indicated on the right.

analyze isolated virions for biotinylated gE (Fig. 3, lane 6). A 1-cm^2 infected monolayer was used to analyze cell lysates for total gE (Fig. 3, lane 7), TGN (lane 9), or TfR (lane 11). One 15-cm^2 infected monolayer was used to analyze isolated virions for total gE (Fig. 3, lane 8), TGN (lane 10), or TfR (lane 12).

The 0-min and 5-h samples in Fig. 3, lanes 1 and 4, showed total cell surface biotinylation of gE. The sample in Fig. 3, lane

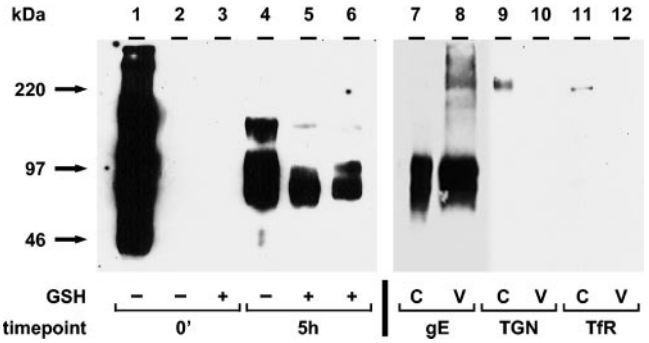

FIG. 3. Incorporation of endocytosed gE into VZV virions. The biotin endocytosis assay was carried out as described in the text. As a control, no biotin was added to the sample in lane 2. Virions were isolated by centrifugation in two KT-glycerol gradients (lanes 6, 8, 10, and 12). Cell lysates were collected before the isolation of virions (lanes 5, 7, 9, and 11). Immunoprecipitated gE samples (lanes 1 to 6) or samples without immunoprecipitation (lanes 7 to 12) were separated by SDS–8% PAGE under nonreducing conditions, and biotinylated glycoproteins were detected with Streptavidin-HRP by Western blotting (lanes 1 to 6). For the detection of total gE (lanes 7 and 8), TGN-46 protein (lanes 9 and 10), or TfR (lanes 11 and 12), protein-specific antibodies were used for Western blotting. C and V indicate cell lysate or virion fraction, respectively. Lanes 1 to 6 and lanes 7 to 12 represent two separate gels. The corresponding molecular mass markers are indicated on the left.

2, without a biotinylation step, was included as a negative control. The 0-min sample in Fig. 3, lane 3, shows that the GSH cleavage step removed all cell surface biotin to an undetectable level. The 5-h sample in Fig. 3, lane 5, was returned to 37°C for 5 h before the cleavage step. As expected from Fig. 2, gE was internalized at 24 hpi and after 5 h of incubation (Fig. 3, lane 5). To determine whether gE retrieved from the cell surface was incorporated into virion particles, isolated virions from the 5-h sample were analyzed for biotinylated gE. As shown in Fig. 3, lane 6, gE endocytosed during the 5-h period was incorporated into virion particles in VZV-infected cells.

Furthermore, the 0-min and 5-h samples in Fig. 3, lanes 1 and 4, showed the coprecipitation of cell surface gE and gI by an anti-gE MAb. The gI band was visible in Fig. 3, lane 4; it was also detected in 5-h samples of a cell lysate (lane 5) and a virion fraction (lane 6) after longer exposures (data not shown). Thus, the results demonstrated not only that gE and gI formed a complex on the cell surface and during endocytosis but also that both glycoproteins were incorporated as a complex into virion particles after endocytosis. In separate experiments (data not shown), we repeated the above experiments but precipitated the samples with an anti-gI MAb and demonstrated directly that gI was retrieved from the cell surface and was incorporated into virions.

As a control for nonvirion gE, we investigated whether a TGN-localized protein, TGN-46 (Fig. 3, lanes 9 and 10), and TfR (lanes 11 and 12) were present in either a cell lysate (lanes 9 and 11) or a virion fraction (lanes 10 and 12). No TGN-46 band was detected in the virion fraction (Fig. 3, lane 10), but it was found in the cell lysate (lane 9). It was previously reported that VZV gE endocytosis mimicked that of TfR (47). Although TfR was detected in the cell lysate (Fig. 3, lane 11), the virion fraction did not contain a TfR band (lane 12).

Incorporation of cell surface biotinylated gH into VZV virions. The next set of experiments was designed to investigate whether endocytosed gH was incorporated into virion particles (Fig. 4). The 0-min sample in Fig. 4, lane 1, showed total cell surface biotinylation of gH. The absence of a glycoprotein band in the 0-min sample in Fig. 4, lane 2, demonstrated that the cleavage step removed all cell surface biotin. The 1-h sample in Fig. 4, lane 3, was returned to 37°C for 1 h before the cleavage step. Endocytosed gH is shown in Fig. 4, lane 3. The viral envelope incorporation assay included samples in Fig. 4, lanes 4 to 8. One 25-cm^2 infected monolayer was used per 0-min sample in Fig. 4, lanes 4 and 5, and per 5-h sample in lane 6. One 35-cm^2 monolayer was used to analyze the cell lysate for biotinylated gH (Fig. 4, lane 7). One 125-cm^2 monolayer was used to analyze isolated virions for biotinylated gH (Fig. 4, lane 8). A 1-cm^2 monolayer was used to analyze the cell lysate for total gH (Fig. 4, lane 9). One 25-cm^2 monolayer was used to determine total gH in isolated virions (Fig. 4, lane 10).

The 0-min and 5-h samples in Fig. 4, lanes 4 and 6, showed total cell surface biotinylation of gH. The absence of a glycoprotein band in the 0-min sample in Fig. 4, lane 5, demonstrated that the GSH cleavage step removed all cell surface biotin. The 5-h sample in Fig. 4, lane 7, was returned to 37°C before the cleavage step. As demonstrated in Fig. 4, lane 7, gH was internalized at 24 hpi and after 5 h of incubation. To determine whether gH retrieved from the cell surface was incorporated into virions, the virion fraction from the 5-h sam-

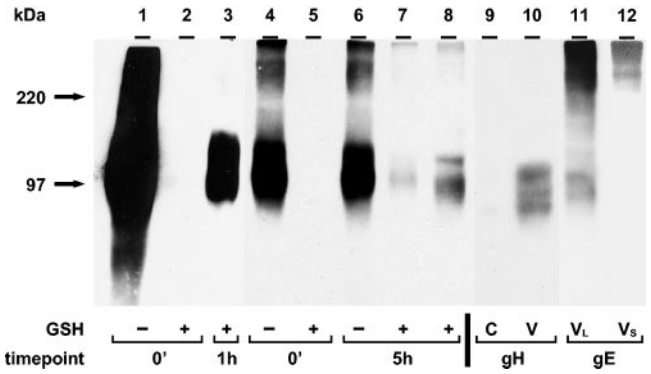

FIG. 4. Incorporation of endocytosed gH into VZV virions. Virions were isolated as described in the legend to Fig. 3 (lanes 8 and 10). Cell lysates were collected before the isolation of virions (lanes 7 and 9). Immunoprecipitated gH samples (lanes 1 to 8) or samples without immunoprecipitation (lanes 9 and 10) were separated by SDS–8% PAGE under nonreducing conditions. Biotinylated glycoproteins were detected with Streptavidin-HRP (lanes 1 to 8). In lanes 9 and 10, Western blotting was performed with an anti-gH MAb. To detect gH-gE complex formation, the nitrocellulose membrane from lane 8 was stripped and probed for a second time with a mouse anti-gE MAb (lane 11). Lane 12 represents a shorter exposure of lane 11 to confirm the migration of the higher-molecular-mass form of gE. V_L and V_S indicate longer and shorter exposures of the virion sample, respectively. Lanes 1 to 3, lanes 4 to 8, and lanes 9 and 10 represent three separate gels. The corresponding molecular mass markers are indicated on the left.

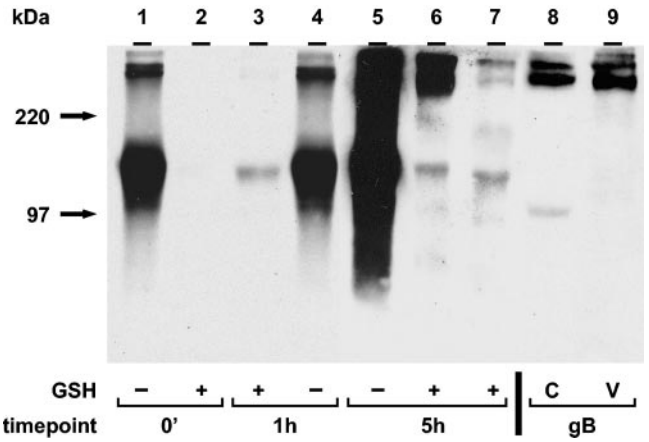

FIG. 5. Incorporation of endocytosed gB into VZV virions. Virions were isolated as described in the legend to Fig. 3 (lanes 7 and 9). Cell lysates were collected before the isolation of virions (lanes 6 and 8). Immunoprecipitated gB samples (lanes 1 to 7) or samples without immunoprecipitation (lanes 8 and 9) were separated by SDS–8% PAGE under nonreducing conditions (lanes 1 to 7) or native conditions (lanes 8 and 9). Biotinylated glycoproteins were detected with Streptavidin-HRP (lanes 1 to 7). In lanes 8 and 9, Western blotting was performed with an anti-gB MAb. Lanes 1 to 4, lanes 5 to 7, and lanes 8 and 9 represent three separate gels. The corresponding molecular mass markers are indicated on the left.

ple in Fig. 4, lane 8, was analyzed and found to be positive for biotinylated gH. The total amounts of gH detected by Western blotting with an anti-gH antibody in cell extracts and virion particles are shown in Fig. 4, lanes 9 and 10, respectively. Like gE, therefore, endocytosed gH was recovered in the virion fraction.

Glycoproteins gE and gH were previously shown to interact during viral glycoprotein trafficking in a transfection system (12) as well as in VZV-infected cells (50). To extend prior observations about gE-gH complex formation, we tested whether gH forms a complex with gE in the virion envelope. The membrane from Fig. 4, lane 8, was stripped after Streptavidin-HRP detection and reprobed with an anti-gE antibody. As shown in Fig. 4, lane 11, a gE protein coprecipitated by a human anti-gH antibody was detected by a mouse anti-gE antibody as a 98-kDa band. Moreover, the reprobed blot with a shorter exposure also identified higher-molecular-mass gE forms among complexes of gE and gH in virions (Fig. 4, lane 12). Thus, the results demonstrated that glycoproteins gE and gH formed a complex not only during their trafficking inside the cell but also during their incorporation into virion particles.

Incorporation of cell surface biotinylated gB into VZV virions. In the next set of experiments, we investigated whether endocytosed gB was incorporated into virion particles (Fig. 5). The 0- and 60-min samples in Fig. 5, lanes 1 and 4, showed total cell surface biotinylation of gB. The absence of a glycoprotein band in Fig. 5, lane 2, demonstrated that the cleavage step removed all cell surface biotin. The sample in Fig. 5, lane 3, indicated that the 140-kDa gB form was endocytosed. In the gB virion incorporation assay (Fig. 5, lanes 5 to 7), we used one 25-cm^2 infected monolayer per 5-h sample in lane 5, one 35-cm^2 monolayer to analyze a cell lysate for biotinylated gB in lane 6, and one 150-cm^2 monolayer to analyze biotinylated gB in isolated virions in lane 7. Total gB was analyzed in a 1-cm^2 monolayer (Fig. 5, lane 8), and total gB in virions was analyzed in one 25-cm^2 monolayer (lane 9). As documented in Fig. 5, lane 7, endocytosed 140-kDa gB as well as higher-molecular-mass gB forms were incorporated into virion particles in VZV-32-infected cells.

The value of using several MAbs is shown by an inspection of Fig. 5. The commercial anti-gB MAb recognized only higher-molecular-mass forms of gB in virion particles (Fig. 5, lane 9) compared to cell lysate samples, where a lower-molecular-mass form was also present (lane 8). The 140-kDa band (Fig. 5, lane 7), representing the form of gB protein incorporated into virion particles, was not detected in virion fraction samples by a commercial anti-gB MAb after immunoblotting (lane 9). There are two explanations. First, different MAbs were used in Fig. 5, lanes 1 to 7 (MAb 158), and lanes 8 and 9 (commercial anti-gB MAb). Second, different conditions were used for SDS-PAGE. Samples in Fig. 5, lanes 1 to 7, were processed under nonreducing conditions and were boiled. On the other hand, only native conditions, without boiling, were used for samples in Fig. 5, lanes 8 and 9. The lack of boiling likely prevented the disaggregation of a gB complex.

High-resolution TEM imaging of biotinylated virions. Earlier studies to define the conditions for the purification of VZV virions were published in 1979 (28). Since that time, there have been advances in high-resolution electron microscopy. In the 1979 studies, the percentages of enveloped particles decreased with successive sedimentations, from 33% in gradient 1 to 18% in gradient 2. Therefore, in this study, we repeated the examination of virions after two sedimentations in KT-glycerol gradients. We postulated that envelopes were being lost during sedimentation. With higher-resolution TEM, we have proven

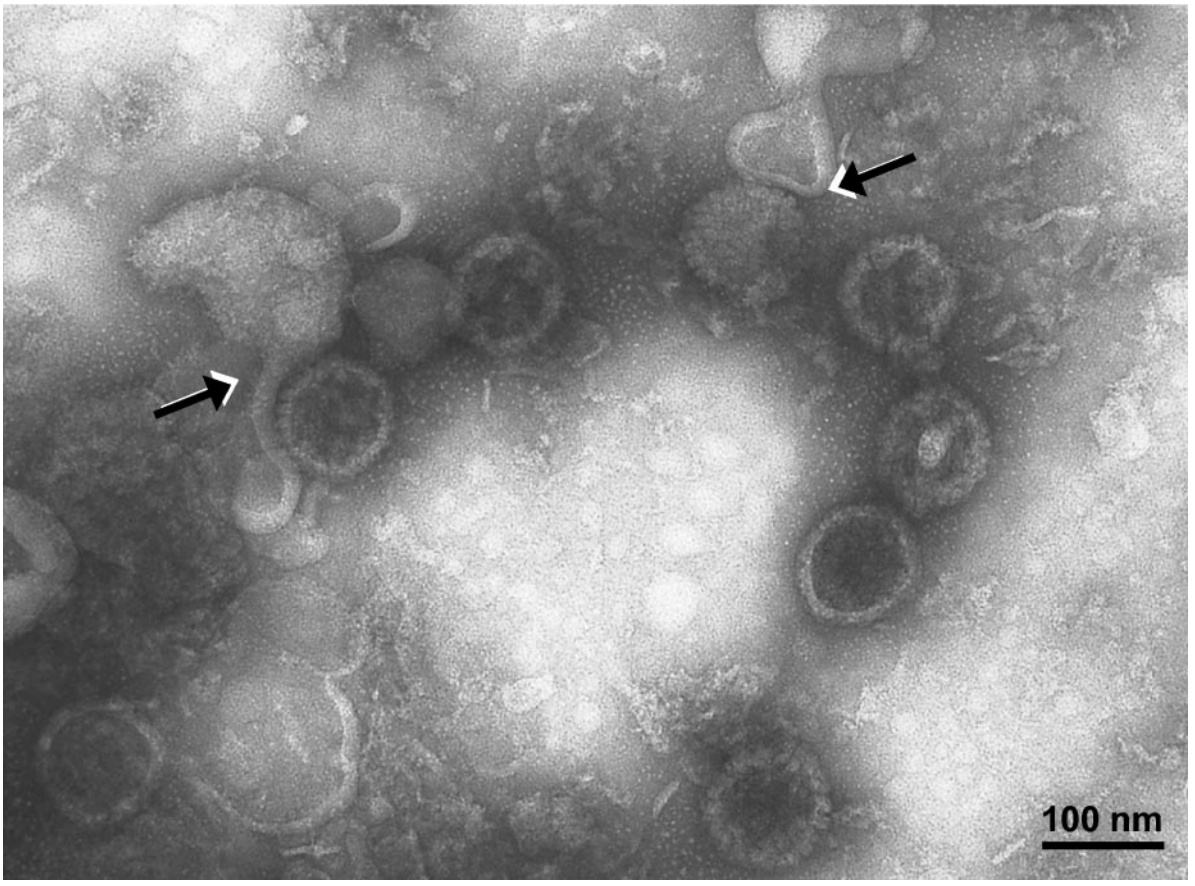

FIG. 6. Virion fraction from the second sedimentation gradient. The virion fraction was processed for TEM as described in the text. Enveloped and nonenveloped particles were easily distinguished. Capsid morphologies were previously described (26). Partially unenveloped virions were seen; in these virions, the envelope had detached from its nucleocapsid (arrows), most likely during centrifugation in two KT-glycerol gradients. The sample was viewed at an accelerating voltage of 75,000 V and at a magnification of ×80,000.

this hypothesis. When the virion band from the second sedimentation was subjected to TEM analysis, the majority of the particles were found to be partially or incompletely enveloped capsids. In Fig. 6, about 10 capsids were clearly delineated. Two of the capsids had partially detached envelopes. Figure 6 also documented our ability to differentiate enveloped virions from naked particles, an important criterion for the next two experiments.

To specifically determine whether biotinylated surface proteins were incorporated into nascent virions, we repeated the gradient sedimentations after the virion envelope incorporation assay. After the second sedimentation, aliquots of VZV virions were labeled with Streptavidin-conjugated gold beads and processed for TEM. Representative micrographs are shown in Fig. 7. Numerous virions labeled with gold beads were easily detected in the samples. Individual gold beads can be seen on each of the envelopes in Fig. 7A. A few gold beads were bound to remnants of envelopes as well. Some complete enveloped particles had as many as five beads (Fig. 7B). Occasionally, enveloped virions were present in small clusters (Fig. 7C). To determine the relative numbers of labeled viruses, all viral particles were counted in multiple fields at a magnification of ×35,000. Among 200 counted viral particles, 27% were positively labeled with one or more gold beads. Since the same percentage of particles was enveloped, the analysis determined that virtually all complete virions contained gold beads on their envelopes.

To prove the specificity of the results shown in Fig. 7, we repeated the biotinylation assay with a goat antibiotin antibody conjugated to ultrasmall gold beads (data not shown). Individual complete virions with gold beads attached to their envelopes were easily found. Altogether, therefore, the TEM results obtained with two different biotin labeling methods confirmed that viral proteins decorated with gold beads were internalized from the cell surface and subsequently were detected on the envelopes of newly formed virions.

DISCUSSION

VZV may be a good model system with which to study the trafficking of glycoproteins prior to virion assembly, since gE endocytosis is an essential function (11, 23, 41). A deenvelopment-reenvelopment model for the acquisition of the final viral envelope has been proposed for VZV (21, 37, 67, 68). An analogous mechanism has been postulated to be involved in the envelopment of PrV and HCMV (9, 20, 22, 51, 52, 59). The model predicts that capsids obtain a primary envelope as they pass through the inner nuclear membrane. As they exit the

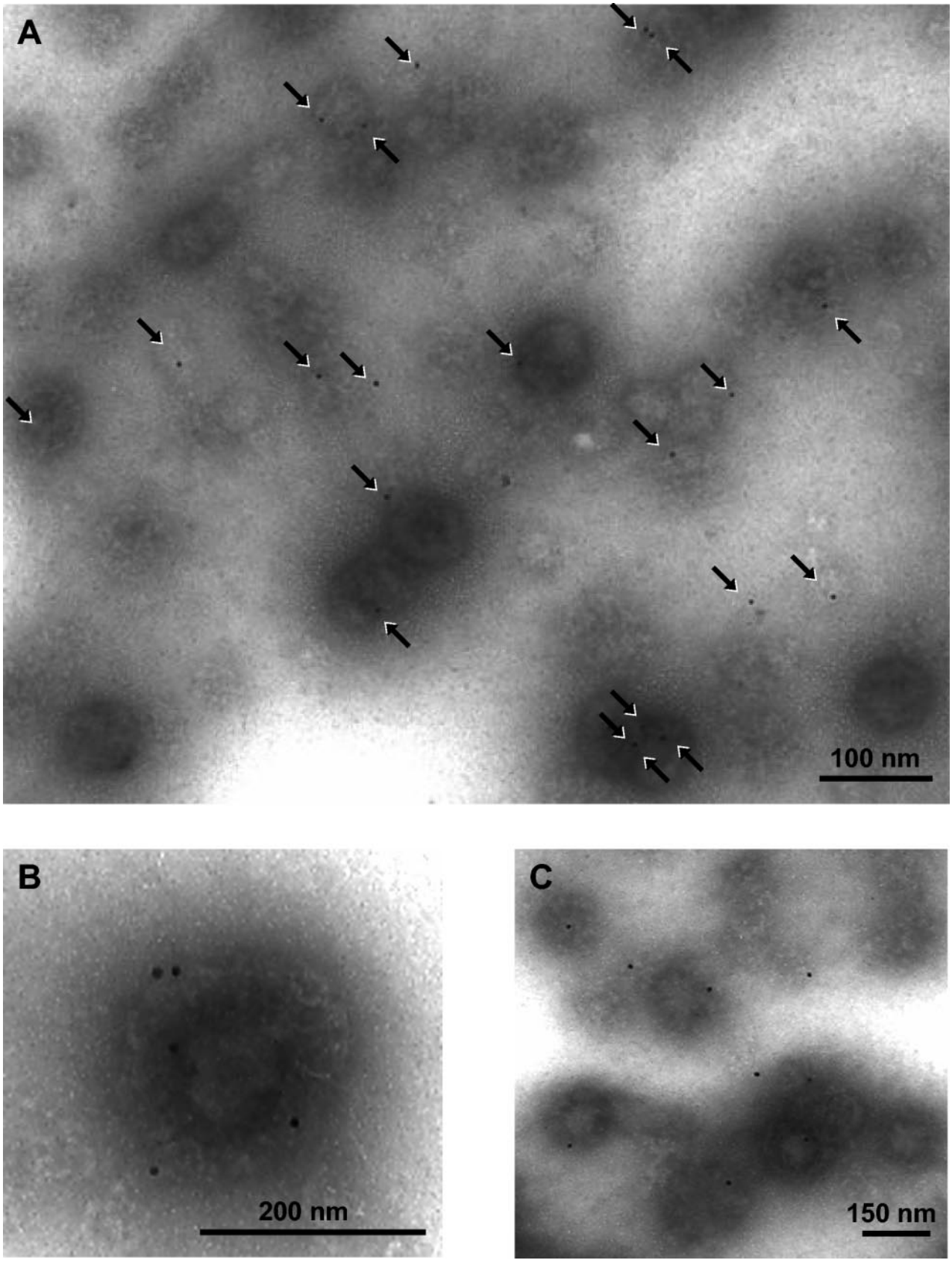

FIG. 7. Virion fractions containing envelopes decorated with Streptavidin-conjugated gold beads. Purified VZV virions from the biotin incorporation assay were processed for TEM after immunostaining was done with Streptavidin-conjugated gold beads as described in Materials and Methods. The arrows indicate the gold beads present on the envelopes of individual complete virions. A few gold beads were present on remnants of detached envelopes as well. The samples were viewed at an accelerating voltage of 75,000 V and at the magnifications indicated by the nanometer bars in panels A, B, and C.

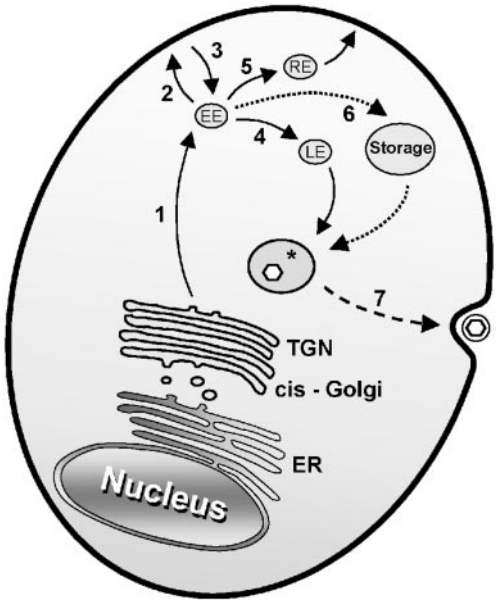

FIG. 8. Trafficking pathways of VZV glycoproteins. The various pathways described in the text are shown. EE, early endosome; LE, late endosome; RE, recycling endosome; Storage, intracellular storage organelle. The asterisk denotes the final virion envelopment compartment derived from the TGN. Enveloped virions within cytoplasmic vacuoles appear on the cell surface after exocytosis.

outer nuclear membrane, they undergo deenvelopment. Capsids released into the cytoplasm are subsequently wrapped by membranes of a post-Golgi compartment, such as the TGN. As previously reported, VZV apparently obtains its final envelope from these TGN vesicles (21, 64, 67, 68). The glycoproteins of VZV are targeted to the TGN and, late in infection, all appear to become concentrated within this organelle (1, 2, 46, 47, 48, 62). Thus, for the assembly of VZV, a high degree of organization is required to localize all of the viral envelope components to the final compartment. TGN sorting implies that TGN targeting signals must be present in the sequences of at least some VZV glycoproteins. Since some VZV glycoproteins contain in their cytosolic domains localization signals that allow these proteins to be targeted to the TGN independently (33, 34, 38, 62), the major aim of the present study was to examine whether endocytosis from the plasma membrane is a substantial pathway by which VZV glycoproteins are delivered to the cytoplasmic compartment for incorporation into virion particles.

Based on cellular protein trafficking pathways, a model for VZV glycoprotein trafficking to the final viral envelopment compartment can be proposed (Fig. 8). Viral glycoproteins synthesized in the TGN are sorted into endosomal vesicles by AP-1 (29). These vesicles traffic to the early endosomes (Fig. 8, pathway 1), from which the glycoproteins can reach the plasma membrane (pathway 2) or remain in the endosomal system (pathway 4). Glycoproteins containing either tyrosine internalization motifs (gE, gB, and gH) or dileucine motifs (gI) are bound at the plasma membrane by AP-2 and are incorporated into clathrin-coated vesicles, which traffic to the early endosomes (Fig. 8, pathway 3). In the early endosomes, the cargo is actively and selectively sorted for transport to the late endosomes (Fig. 8, pathway 4) or to the recycling endosomes (pathway 5). VZV glycoproteins, based on their cytoplasmic tail domains, are expected to follow similar pathways, whose final destination is presumed to be the site of virion assembly (Fig. 8). In contrast to what has been reported for PrV glycoproteins (14, 15, 16, 58), antibody binding is not a critical mechanism by which VZV glycoproteins are internalized (49). Rather than immune evasion, therefore, we postulate that endocytosis is an important trafficking mechanism by which glycoproteins are delivered to the site of assembly.

The recent report about the lethality of a recombinant VZV containing only one mutation in one gene, namely, the endocytosis motif of gE, strongly supports the conclusion that endocytosis is an essential element of the VZV life cycle (41). Earlier reports suggested a preeminent role of gE in glycoprotein trafficking. gE not only interacts with gI but also associates with gH during postendocytosis trafficking; interestingly, the recently described gE-gH complex was also found in the virion envelope (50). These data supported a mechanism of gE-gH complex formation as a means by which gH was shuttled to the TGN after internalization through the other trafficking motifs in the long gE tail. Presumably, if VZV gE internalization is disrupted, then the trafficking of both gI and gH also is disrupted, an apparently lethal event in the VZV life cycle. Based on the results obtained in this study, we propose that gE, gI, and gH in the lethal recombinant VZV fail to reach the cytoplasmic site of virion envelopment in adequate amounts or correct compositions. As a corollary, these comparisons further suggest that VZV, with its relatively small number of glycoproteins, has fewer trafficking options during envelopment than other herpesviruses. For example, when the role of endocytosis in PrV envelopment was investigated by Tirabassi and Enquist (57, 58), biotinylation studies demonstrated that PrV gE was endocytosed at 4 hpi. However, little biotinylated gE was found in virion particles 12 h later. The VZV results were completely different from those for PrV in that a majority of enveloped VZV virions contained internalized biotinylated glycoproteins. Thus, PrV may have alternative pathways for glycoprotein transport during envelopment, since PrV with a gE endocytosis motif mutation is able to replicate, albeit with a small-plaque phenotype.

A role for gB endocytosis in the biogenesis of other herpesviruses, besides VZV, was proposed previously. HCMV gB, a major component of the HCMV envelope, is essential for the production of infectious virus. Surface biotinylation of HCMV-infected human fibroblasts demonstrated that a major fraction of internalized gB was found subsequently in HCMV virions (51). In addition, endocytosis of gB was shown to play a role in mediating the TGN localization of gB and in targeting of the protein to the site of virus envelopment in HCMV-infected astrocytoma cells (36). However, prevention of endocytosis by the expression of a dominant-negative dynamin mutant did not affect the production of infectious virus. Endocytosis and envelopment have also been investigated in an HSV-1 system. When endocytosis-deficient gB molecules were expressed with a gB-null virus, infectivity was markedly reduced (5). Thus, there are unresolved differences between HCMV and HSV-1 data, with regard to whether endocytosed gB is essential for the formation of infectious virions.

There is one additional issue to address, namely, the conse-

quences of the endocytosis block late in infection. The first possibility is that viral glycoproteins internalized early in infection remain in a storage compartment until they are sorted to the TGN virion assembly vacuole (Fig. 8, pathway 6). This pathway was suggested in earlier reports (51, 58). An alternative possibility is that virions formed early in infection contain a subset of glycoproteins different from those contained in virions assembled later in infection. In this scenario, early virions would contain primarily glycoproteins internalized from the cell surface, while later virions would contain glycoproteins shuttled to the TGN assembly site from the early endosomal pathway without the intermediate steps of transport to and internalization from the cell surface (Fig. 8, pathways 1 and 4). Again, the data from lethal recombinant VZV gE are instructive; unlike other herpesviruses, VZV apparently cannot use an alternative trafficking pathway if the gE endocytosis pathway is blocked by a mutation in the YAGL sequence in the gE cytoplasmic tail. For VZV and in contradistinction to PrV, therefore, endocytosis is a glycoprotein trafficking mechanism of paramount importance.

ACKNOWLEDGMENTS

This research was supported by NIH grant RO1 AI22795 (to C.G.); a fellowship award from the VZV Research Foundation, New York, N.Y. (to L.M.); a stipend from the Iowa Biosciences Advantage Program (NIH R25 GM 58939; to E.H.); and an Infectious Diseases Training fellowship (NIH R32 AI 07343; to E.G.).

REFERENCES

1. **Alconada, A., U. Bauer, L. Baudoux, J. Piette, and B. Hoflack.** 1998. Intracellular transport of the glycoproteins gE and gI of the varicella-zoster virus. gE accelerates the maturation of gI and determines its accumulation in the trans-Golgi network. J. Biol. Chem. **273:**13430–13436.
2. **Alconada, A., U. Bauer, and B. Hoflack.** 1996. A tyrosine-based motif and a casein kinase II phosphorylation site regulate the intracellular trafficking of the varicella-zoster virus glycoprotein I, a protein localized in the trans-Golgi network. EMBO J. **15:**6096–6110.
3. **Alconada, A., U. Bauer, B. Sodeik, and B. Hoflack.** 1999. Intracellular traffic of herpes simplex virus glycoprotein gE: characterization of the sorting signals required for its *trans*-Golgi network localization. J. Virol. **73:**377–387.
4. **Asano, Y., and M. Takahashi.** 1980. Studies on the polypeptides of varicella-zoster (V-Z) virus. II. Syntheses of viral polypeptides in infected cells. Biken J. **23:**95–106.
5. **Beitia Ortiz de Zarate, I., K. Kaelin, and F. Rozenberg.** 2004. Effects of mutations in the cytoplasmic domain of herpes simplex virus type 1 glycoprotein B on intracellular transport and infectivity. J. Virol. **78:**1540–1551.
6. **Bonifacino, J. S., and E. C. Dell'Angelica.** 1999. Molecular bases for the recognition of tyrosine-based sorting signals. J. Cell Biol. **145:**923–926.
7. **Bretscher, M. S., and R. Lutter.** 1988. A new method for detecting endocytosed proteins. EMBO J. **7:**4087–4092.
8. **Brideau, A. D., L. W. Enquist, and R. S. Tirabassi.** 2000. The role of virion membrane protein endocytosis in the herpesvirus life cycle. J. Clin. Virol. **17:**69–82.
9. **Card, J. P., L. Rinaman, R. B. Lynn, B. H. Lee, R. P. Meade, R. R. Miselis, and L. W. Enquist.** 1993. Pseudorabies virus infection of the rat central nervous system: ultrastructural characterization of viral replication, transport, and pathogenesis. J. Neurosci. **13:**2515–2539.
10. **Crump, C. M., Y. Xiang, L. Thomas, F. Gu, C. Austin, S. A. Tooze, and G. Thomas.** 2001. PACS-1 binding to adaptors is required for acidic cluster motif-mediated protein traffic. EMBO J. **20:**2191–2201.
11. **Davison, A. J., and J. E. Scott.** 1986. The complete DNA sequence of varicella-zoster virus. J. Gen. Virol. **67:**1759–1816.
12. **Duus, K. M., and C. Grose.** 1996. Multiple regulatory effects of varicella-zoster virus (VZV) gL on trafficking patterns and fusogenic properties of VZV gH. J. Virol. **70:**8961–8971.
13. **Duus, K. M., C. Hatfield, and C. Grose.** 1995. Cell surface expression and fusion by the varicella-zoster virus gH:gL glycoprotein complex: analysis by laser scanning confocal microscopy. Virology **210:**429–440.
14. **Favoreel, H. W., H. J. Nauwynck, H. M. Halewyck, P. Van Oostveldt, T. C. Mettenleiter, and M. B. Pensaert.** 1999. Antibody-induced endocytosis of viral glycoproteins and major histocompatibility complex class I on pseudorabies virus-infected monocytes. J. Gen. Virol. **80:**1283–1291.
15. **Favoreel, H. W., H. J. Nauwynck, P. Van Oostveldt, and M. B. Pensaert.** 2000. Role of anti-gB and -gD antibodies in antibody-induced endocytosis of viral and cellular cell surface glycoproteins expressed on pseudorabies virus-infected monocytes. Virology **267:**151–158.
16. **Favoreel, H. W., G. Van Minnebruggen, H. J. Nauwynck, L. W. Enquist, and M. B. Pensaert.** 2002. A tyrosine-based motif in the cytoplasmic tail of pseudorabies virus glycoprotein B is important for both antibody-induced internalization of viral glycoproteins and efficient cell-to-cell spread. J. Virol. **76:**6845–6851.
17. **Fish, K. N., C. Soderberg-Naucler, and J. A. Nelson.** 1998. Steady-state plasma membrane expression of human cytomegalovirus gB is determined by the phosphorylation state of Ser900. J. Virol. **72:**6657–6664.
18. **Fraile-Ramos, A., T. N. Kledal, A. Pelchen-Matthews, K. Bowers, T. W. Schwartz, and M. Marsh.** 2001. The human cytomegalovirus US28 protein is located in endocytic vesicles and undergoes constitutive endocytosis and recycling. Mol. Biol. Cell **12:**1737–1749.
19. **Fraile-Ramos, A., A. Pelchen-Matthews, T. N. Kledal, H. Browne, T. W. Schwartz, and M. Marsh.** 2002. Localization of HCMV UL33 and US27 in endocytic compartments and viral membranes. Traffic **3:**218–232.
20. **Fuchs, W., B. G. Klupp, H. Granzow, H. J. Rziha, and T. C. Mettenleiter.** 1996. Identification and characterization of the pseudorabies virus UL3.5 protein, which is involved in virus egress. J. Virol. **70:**3517–3527.
21. **Gershon, A. A., D. L. Sherman, Z. Zhu, C. A. Gabel, R. T. Ambron, and M. D. Gershon.** 1994. Intracellular transport of newly synthesized varicella-zoster virus: final envelopment in the *trans*-Golgi network. J. Virol. **68:**6372–6390.
22. **Granzow, H., F. Weiland, A. Jons, B. G. Klupp, A. Karger, and T. C. Mettenleiter.** 1997. Ultrastructural analysis of the replication cycle of pseudorabies virus in cell culture: a reassessment. J. Virol. **71:**2072–2082.
23. **Grose, C.** 2002. The predominant varicella-zoster virus gE and gI glycoprotein complex, p. 195–223. *In* A. Holzenburg and E. Bogner (ed.), Structure-function relationships of human pathogenic viruses. Kluwer Academic Press, Inc., New York, N.Y.
24. **Grose, C., and P. A. Brunell.** 1978. Varicella-zoster virus: isolation and propagation in human melanoma cells at 36 and 32°C. Infect. Immun. **19:**199–203.
25. **Grose, C., D. P. Edwards, W. E. Friedrichs, K. A. Weigle, and W. L. McGuire.** 1983. Monoclonal antibodies against three major glycoproteins of varicella-zoster virus. Infect. Immun. **40:**381–388.
26. **Grose, C., R. Harson, and S. Beck.** 1995. Computer modeling of prototypic and aberrant nucleocapsids of varicella-zoster virus. Virology **214:**321–329.
27. **Grose, C., W. Jackson, and J. A. Traugh.** 1989. Phosphorylation of varicella-zoster virus glycoprotein gpI by mammalian casein kinase II and casein kinase I. J. Virol. **63:**3912–3918.
28. **Grose, C., D. M. Perrotta, P. A. Brunell, and G. C. Smith.** 1979. Cell-free varicella-zoster virus in cultured human melanoma cells. J. Gen. Virol. **43:**15–27.
29. **Gu, F., C. M. Crump, and G. Thomas.** 2001. trans-Golgi network sorting. Cell. Mol. Life Sci. **58:**1067–1084.
30. **Harson, R., and C. Grose.** 1995. Egress of varicella-zoster virus from the melanoma cell: a tropism for the melanocyte. J. Virol. **69:**4994–5010.
31. **Harter, C., and I. Mellman.** 1992. Transport of the lysosomal membrane glycoprotein lgp120 (lgp-A) to lysosomes does not require appearance on the plasma membrane. J. Cell Biol. **117:**311–325.
32. **Hatfield, C., K. M. Duus, J. Chen, D. H. Jones, and C. Grose.** 1997. Epitope mapping and tagging by recombination PCR mutagenesis. BioTechniques **22:**332–337.
33. **Heineman, T. C., and S. L. Hall.** 2002. Role of the varicella-zoster virus gB cytoplasmic domain in gB transport and viral egress. J. Virol. **76:**591–599.
34. **Heineman, T. C., and S. L. Hall.** 2001. VZV gB endocytosis and Golgi localization are mediated by YXXphi motifs in its cytoplasmic domain. Virology **285:**42–49.
35. **Heineman, T. C., N. Krudwig, and S. L. Hall.** 2000. Cytoplasmic domain signal sequences that mediate transport of varicella-zoster virus gB from the endoplasmic reticulum to the Golgi. J. Virol. **74:**9421–9430.
36. **Jarvis, M. A., K. N. Fish, C. Soderberg-Naucler, D. N. Streblow, H. L. Meyers, G. Thomas, and J. A. Nelson.** 2002. Retrieval of human cytomegalovirus glycoprotein B from cell surface is not required for virus envelopment in astrocytoma cells. J. Virol. **76:**5147–5155.
37. **Jones, F., and C. Grose.** 1988. Role of cytoplasmic vacuoles in varicella-zoster virus glycoprotein trafficking and virion envelopment. J. Virol. **62:**2701–2711.
38. **Kenyon, T. K., J. I. Cohen, and C. Grose.** 2002. Phosphorylation by the varicella-zoster virus ORF47 protein serine kinase determines whether endocytosed viral gE traffics to the *trans*-Golgi network or recycles to the cell membrane. J. Virol. **76:**10980–10993.
39. **Mallory, S., M. Sommer, and A. M. Arvin.** 1997. Mutational analysis of the role of glycoprotein I in varicella-zoster virus replication and its effects on glycoprotein E conformation and trafficking. J. Virol. **71:**8279–8288.
40. **Marsh, M., and A. Pelchen-Matthews.** 2000. Endocytosis in viral replication. Traffic **1:**525–532.
41. **Moffat, J., C. Mo, J. J. Cheng, M. Sommer, L. Zerboni, S. Stamatis, and**

A. M. Arvin. 2004. Functions of the C-terminal domain of varicella-zoster virus glycoprotein E in viral replication in vitro and skin and T-cell tropism in vivo. J. Virol. **78:**12406–12415.
42. **Montalvo, E. A., and C. Grose.** 1986. Neutralization epitope of varicella zoster virus on native viral glycoprotein gp118 (VZV gH). Virology **149:**230–241.
43. **Montalvo, E. A., and C. Grose.** 1986. Varicella zoster virus glycoprotein gpI (gE) is selectively phosphorylated by a virus-induced protein kinase. Proc. Natl. Acad. Sci. USA **83:**8967–8971.
44. **Montalvo, E. A., R. T. Parmley, and C. Grose.** 1985. Structural analysis of the varicella-zoster virus gp98-gp62 complex: posttranslational addition of N-linked and O-linked oligosaccharide moieties. J. Virol. **53:**761–770.
45. **Olson, J. K., G. A. Bishop, and C. Grose.** 1997. Varicella-zoster virus Fc receptor gE glycoprotein: serine/threonine and tyrosine phosphorylation of monomeric and dimeric forms. J. Virol. **71:**110–119.
46. **Olson, J. K., and C. Grose.** 1998. Complex formation facilitates endocytosis of the varicella-zoster virus gE:gI Fc receptor. J. Virol. **72:**1542–1551.
47. **Olson, J. K., and C. Grose.** 1997. Endocytosis and recycling of varicella-zoster virus Fc receptor glycoprotein gE: internalization mediated by a YXXL motif in the cytoplasmic tail. J. Virol. **71:**4042–4054.
48. **Olson, J. K., R. A. Santos, and C. Grose.** 1998. Varicella-zoster virus glycoprotein gE: endocytosis and trafficking of the Fc receptor. J. Infect. Dis. **178**(Suppl. 1)**:**S2–S6.
49. **Pasieka, T. J., L. Maresova, and C. Grose.** 2003. A functional YNKI motif in the short cytoplasmic tail of varicella-zoster virus glycoprotein gH mediates clathrin-dependent and antibody-independent endocytosis. J. Virol. **77:**4191–4204.
50. **Pasieka, T. J., L. Maresova, K. Shiraki, and C. Grose.** 2004. Regulation of varicella-zoster virus-induced cell-to-cell fusion by the endocytosis-competent glycoproteins gH and gE. J. Virol. **78:**2884–2896.
51. **Radsak, K., M. Eickmann, T. Mockenhaupt, E. Bogner, H. Kern, A. Eis-Hubinger, and M. Reschke.** 1996. Retrieval of human cytomegalovirus glycoprotein B from the infected cell surface for virus envelopment. Arch. Virol. **141:**557–572.
52. **Sanchez, V., K. D. Greis, E. Sztul, and W. J. Britt.** 2000. Accumulation of virion tegument and envelope proteins in a stable cytoplasmic compartment during human cytomegalovirus replication: characterization of a potential site of virus assembly. J. Virol. **74:**975–986.
53. **Santos, R. A., C. C. Hatfield, N. L. Cole, J. A. Padilla, J. F. Moffat, A. M. Arvin, W. T. Ruyechan, J. Hay, and C. Grose.** 2000. Varicella-zoster virus gE escape mutant VZV-MSP exhibits an accelerated cell-to-cell spread phenotype in both infected cell cultures and SCID-hu mice. Virology **275:**306–317.
54. **Santos, R. A., J. A. Padilla, C. Hatfield, and C. Grose.** 1998. Antigenic variation of varicella zoster virus Fc receptor gE: loss of a major B-cell epitope in the ectodomain. Virology **249:**21–31.
55. **Scott, G. K., F. Gu, C. M. Crump, L. Thomas, L. Wan, Y. Xiang, and G. Thomas.** 2003. The phosphorylation state of an autoregulatory domain controls PACS-1-directed protein traffic. EMBO J. **22:**6234–6244.
56. **Sugano, T., T. Tomiyama, Y. Matsumoto, S. Sasaki, T. Kimura, B. Forghani, and Y. Masuho.** 1991. A human monoclonal antibody against varicella-zoster virus glycoprotein III. J. Gen. Virol. **72:**2065–2073.
57. **Tirabassi, R. S., and L. W. Enquist.** 1999. Mutation of the YXXL endocytosis motif in the cytoplasmic tail of pseudorabies virus gE. J. Virol. **73:**2717–2728.
58. **Tirabassi, R. S., and L. W. Enquist.** 1998. Role of envelope protein gE endocytosis in the pseudorabies virus life cycle. J. Virol. **72:**4571–4579.
59. **Tooze, J., M. Hollinshead, B. Reis, K. Radsak, and H. Kern.** 1993. Progeny vaccinia and human cytomegalovirus particles utilize early endosomal cisternae for their envelopes. Eur. J. Cell Biol. **60:**163–178.
60. **Tugizov, S., E. Maidji, J. Xiao, and L. Pereira.** 1999. An acidic cluster in the cytosolic domain of human cytomegalovirus glycoprotein B is a signal for endocytosis from the plasma membrane. J. Virol. **73:**8677–8688.
61. **Wan, L., S. S. Molloy, L. Thomas, G. Liu, Y. Xiang, S. L. Rybak, and G. Thomas.** 1998. PACS-1 defines a novel gene family of cytosolic sorting proteins required for trans-Golgi network localization. Cell **94:**205–216.
62. **Wang, Z., M. D. Gershon, O. Lungu, C. A. Panagiotidis, Z. Zhu, Y. Hao, and A. A. Gershon.** 1998. Intracellular transport of varicella-zoster glycoproteins. J. Infect. Dis. **178**(Suppl. 1)**:**S7–S12.
63. **Wang, Z. H., M. D. Gershon, O. Lungu, Z. Zhu, and A. A. Gershon.** 2000. Trafficking of varicella-zoster virus glycoprotein gI: T(338)-dependent retention in the *trans*-Golgi network, secretion, and mannose 6-phosphate-inhibitable uptake of the ectodomain. J. Virol. **74:**6600–6613.
64. **Wang, Z. H., M. D. Gershon, O. Lungu, Z. Zhu, S. Mallory, A. M. Arvin, and A. A. Gershon.** 2001. Essential role played by the C-terminal domain of glycoprotein I in envelopment of varicella-zoster virus in the *trans*-Golgi network: interactions of glycoproteins with tegument. J. Virol. **75:**323–340.
65. **Yao, Z., and C. Grose.** 1994. Unusual phosphorylation sequence in the gpIV (gI) component of the varicella-zoster virus gpI-gpIV glycoprotein complex (VZV gE-gI complex). J. Virol. **68:**4204–4211.
66. **Yao, Z., W. Jackson, and C. Grose.** 1993. Identification of the phosphorylation sequence in the cytoplasmic tail of the varicella-zoster virus Fc receptor glycoprotein gpI. J. Virol. **67:**4464–4473.
67. **Zhu, Z., M. D. Gershon, Y. Hao, R. T. Ambron, C. A. Gabel, and A. A. Gershon.** 1995. Envelopment of varicella-zoster virus: targeting of viral glycoproteins to the *trans*-Golgi network. J. Virol. **69:**7951–7959.
68. **Zhu, Z., Y. Hao, M. D. Gershon, R. T. Ambron, and A. A. Gershon.** 1996. Targeting of glycoprotein I (gE) of varicella-zoster virus to the *trans*-Golgi network by an AYRV sequence and an acidic amino acid-rich patch in the cytosolic domain of the molecule. J. Virol. **70:**6563–6575.